

Looking at Extremes with Laser Velocimetry

**James F. Meyers
NASA - Langley Research Center
Hampton, Virginia 23681**

**11th International Invitational Symposium
on the
Unification of Analytical, Computational,
and Experimental Solution Methodologies
August 18-20, 1993
Danvers, Massachusetts**

Looking at Extremes with Laser Velocimetry

James F. Meyers
Senior Electronics Engineer
Mail Stop 235A
NASA Langley Research Center
Hampton, Virginia 23681, U.S.A.

Abstract

The capability of laser velocimetry techniques to measure extremes in fluid dynamics is demonstrated. Examples requiring accurate measurements of intricate flows include investigations of Görtler vortices within a laminar boundary layer along the concave surface of a super critical airfoil, and the buoyancy effects within the flow above a hot susceptor in a Chemical Vapor Deposition Reactor. At the opposite end of the measurement spectrum, global velocity measurements of supersonic flows above an inclined flat plate and a 75-degree delta wing were made with Doppler global velocimetry.

Nomenclature

C_p	pressure coefficient
c	chord length
i, j, k	unit vectors in the streamwise, crosswise, and vertical directions, respectively
M_∞	free-stream Mach number
R_c	Reynolds number based on chord
U, V, W	velocity in the streamwise, crosswise, and vertical directions, respectively
V_∞	free-stream velocity
x, y, z	model coordinates in the streamwise, crosswise, and vertical directions, respectively
α	light sheet angle above horizontal plane

Introduction

Although laser velocimetry is becoming a routine measurement tool for flow field diagnostics, its capabilities to measure intricate, highly detailed flows are not typically employed. The perception that detailed three-component measurements are very difficult, and require expensive equipment has minimized its use on entire classes of flows. Unfortunately, many of these flows, e.g., boundary layers, and very low and very high speed flows, are fundamental to the understanding of detailed flow characteristics needed in a variety of engineering applications, from semiconductor furnaces to advanced aircraft.

The intent of the present paper is to describe several flow field investigations conducted at Langley Research Center, which illustrate the capabilities of laser velocimetry to perform detailed measurements at the extremes of flow conditions. The minute details of Görtler vortices within a laminar boundary layer were investigated using a specialized, single-axis, three-component fringe-type laser velocimeter. The entire flow was contained within the 2 mm-thick boundary layer above the model surface. In the next example, additional complexities were imposed on the laser velocimetry system when measurements were made inside a hand-blown glass Chemical Vapor Deposition Reactor. The difficulties of operating an orthogonal, three-component system within reactive flows about an RF heated graphite susceptor were overcome to produce the first detailed measurements showing the influence of thermal buoyancy on the flow.

At the opposite end of the velocity spectrum is supersonic flow. Application of classic fringe-type laser velocimetry to high-speed flows is limited by the long acquisition times required for sufficient statistical fidelity, as compared with the typically short tunnel run times. Global velocimetry techniques, such as particle image velocimetry and Doppler global velocimetry, overcome this limitation by instantaneously measuring the entire flow field. However, particle image velocimetry requires large particles, which may not faithfully track the flow. Doppler global velocimetry, on the other hand, can use condensed water vapor to provide measurements that should accurately represent the velocity flow field. Examples of supersonic measurements include flow field investigations about an oblique shock above an inclined flat plate, and the vortical flow field above a 75-degree delta wing.

Measurement of the Görtler Instability on an Airfoil

Counter-rotating streamwise vortices arise in boundary layers along concave surfaces due to centrifugal effects.¹ These Görtler vortices can couple with Tollmien-Schlichting waves and crossflow vortices to trigger early transition to turbulence. Understanding these interactions may provide the insight necessary to design efficient supercritical laminar-flow-control wings.

The investigation of Görtler vortices was conducted above a 1.83-meter chord airfoil inversely mounted in the NASA Langley Low-Turbulence Pressure Tunnel (LTPT).² A photograph of the model is shown in figure 1. The primary area of interest was the concave region from $x/c = 0.175$ to $x/c = 0.275$. The region had a minimum radius of curvature of 0.24 m. The laminar boundary layer was held attached to the concave region using suction through a 0.11- x 0.76-m perforated titanium panel located in the compression part of the region. A 10-percent chord flap was used to control the stagnation point location to maintain a flat or slightly favorable pressure gradient ahead of the concave region. The pressure distribution along the wing is shown in figure 2.

The LTPT was a pressurized, closed-circuit, continuous flow wind tunnel. The test section was 2.29 m high, 2.29 m long, and 0.91 m wide. The contraction ratio was 17.6. The tunnel had excellent flow quality due, in part, to the nine screens in the settling chamber. The velocity fluctuations in the test section were found to be 0.025 percent at 0.05 Mach number using hot wire anemometry.³ The pressure fluctuations at the test section wall, normalized with respect to free-stream pressure, were $\sim 10^{-5}$ at this Mach number. The tunnel was operated at atmospheric pressure to relax the requirement of environmental isolation of the laser velocimeter located in the plenum chamber. The chord Reynolds number was varied from 1.0 million to 5.9 million and the Mach number was adjusted from 0.024 to 0.125.

The test requirements of single-window access and an extremely small sample volume were satisfied by developing a specialized single-axis three-component system using the five-beam optical configuration, figure 3.⁴ The system used the standard diamond pattern with the 514.5 nm beams arranged horizontally, and 488.0 nm beams arranged vertically to measure the U or streamwise component and the V or vertical component respectively. A third green beam was aligned along the optical axis to form two additional fringe patterns as it interfered with the U component beams. These additional fringe patterns were inclined symmetrically with respect to the optical axis yielding equal contributions of the U component and equal, but opposite,

contributions of the W or spanwise velocity component. The signals obtained from the three green fringe patterns were isolated using Bragg cells placed in the U component beams to offset each signal baseline frequency. A network of electronic double-balanced mixers and filters separated the individual signals for processing in standard high-speed burst counters. The individual beams were expanded prior to focusing to reduce the measurement volume diameter to 40 microns. The flow was seeded with tridecane particles generated with a standard spray-type atomizer.

The first part of the test program concentrated on the determination of whether Görtler vortices could be formed within the concave region incorporated in the model, and if the suction region would hold the vortices within the boundary layer in a stable manner. Visualization of the vortex tracks on the surface could be obtained by spraying a thin layer of solid white biphenyl material over the black model surface. The differential surface shear stress distribution under the layer of counter-rotating Görtler vortices increased the heat transfer at the airfoil surface, sublimating the hydrocarbon material and marking the vortex paths. Elapsed times from 30 minutes to 1 hour were required to develop a clearly delineated pattern, figure 4. The dark bands represent the high shear stress regions whereas the white bands correspond to low shear regions. A set of black and white bands constitutes a pair of counter-rotating Görtler vortices.

The small size and low velocities expected within the Görtler vortices require extreme velocity sensitivity in the laser velocimeter. Expanding the laser beams to provide a 40-micron diameter measurement volume, coupled with a 15-degree cross-beam angle provided the necessary characteristics. Test results indicated that the greatest change in velocity occurred in the streamwise component, thus providing the greatest potential for determining the location of the vortex core. Plotting the measured streamwise velocity as a function of span distance, figure 5, showed a curious decrease of velocity with increased span distance. This decrease in velocity was traced to minute deflections of the floor supporting the heavy laser optics traverse mechanism, causing the measurement volume to move deeper into the boundary layer as it was moved along the span. The maximum deflection was measured to be 0.18 mm.

Full plane velocity measurements were made at x/c distances from 0.15 to 0.3 at every 0.025 x/c for Mach 0.024 and Mach 0.05. An example data set taken at Mach 0.05 is shown in figure 6 for an x/c distance of 0.275. Except where secondary instability was present, the separation between the vortex pairs did not vary by more than 10 percent throughout the measurement zone at a given free stream condition.

Vortex separation distances found with the laser velocimeter agreed well with those observed using the surface flow visualization technique.

Flow Field Measurements in the Chemical Vapor Deposition Facility

An effort to characterize the fluid dynamics of nonisothermal, chemically reactive flows of gaseous mixtures inside fused silica Chemical Vapor Deposition (CVD) reactor vessels has been underway at the NASA Langley Research Center for a number of years.⁵ This effort concentrates on the determination of buoyancy effects within the reactive flow, and the development of an experimental database from a matrix of test conditions to serve as verification for theoretical simulations of the reactive flows. The goal is to determine if microgravity conditions will improve the layer thickness and compositional uniformity, the abruptness of alloy interfaces, and the growth efficiency. The main tool in the experimental characterization is an orthogonal three-component fringe-type laser velocimeter specifically adapted for measurements within hand-blown chambers used for crystal growth and film formation by CVD, figure 7.⁶

The CVD process is extremely important for its use in the production of electronic semiconductor components, thin films, and coatings for optical elements. Generally, CVD involves the use of a carrier gas such as hydrogen to transport chemically reactive source material to locations where the deposition of solid layers is desired. The chemically active region is normally a hot zone on a susceptor where reactions occur which release the desired deposition material. The entire process is confined within special chambers called reactors which are usually constructed of hand-blown fused silica. Unfortunately, most CVD reactors are based on designs obtained through trial-and-error and not on fundamental fluid mechanics. The current effort represents one of the few methodical investigations of these complicated flows. It is also one of the only efforts to develop measurement technologies for the characterization of CVD reactors in space.

Characterization of the fluid dynamics inside a CVD reactor using standard probe techniques, such as hot wires or pitot probes, is normally restricted by the hazardous gases, high temperatures and limited experimental access which are characteristic of most CVD systems. Optical techniques, such as flow visualization and laser velocimetry, have had greater success and should provide excellent measurement accuracy.

The classic question of whether the motion of small tracer particles would match the gas flow, should not be a concern with typical flow velocities less than 1 m/sec. Unfortunately, Stokes drag force is not the only force acting on a particle in nonisothermal flows. An additional force causes the particle trajectory to deviate from the true gas streamline when it passes through a thermal gradient. The magnitude of this thermophoretic force is determined by the strength of the thermal gradient, the size of the particle, and the thermophysical properties of both the particle and the gas. The results of several investigations characterizing this effect indicate that the utility of particle-based velocimetry techniques to quantify gas fluid dynamics in strong thermal gradients is questionable.^{7, 8} However, the present effort at Langley demonstrates that current particle-based velocimetry instrumentation can be employed to characterize significant portions of many nonisothermal flow fields despite this valid concern.

As an example of the fluid dynamics investigated in CVD, the flow within a fused silica reactor used for GaAs growth will be examined.⁵ The reactor was designed to operate in a horizontal cylindrical tube configuration, figure 8. Instead of the usual hemispherical inlet section, the front end of this reactor consisted of a flat, elliptical plate welded to the circular cylinder at 31 degrees to the axis of the cylinder. The inlet tube for the gas supply was blended into the joint at the bottom of the cylinder and aligned with the major axis of the elliptical plate. The growth region on the face of the graphite susceptor was also slanted at 31 degrees to the cylinder axis, thus forming a uniform gap between the susceptor and the reactor front face.

Nitrogen gas seeded with 1.3 micron latex particles from a commercial nebulizer was used as the test gas. The hydrogen carrier gas normally used with this reactor could not be used for these tests due to safety constraints imposed by the available particle injection system. The locations of the measurement stations were selected to provide data at regular spatial locations in planes parallel to and at specific distances from the face of the graphite susceptor. No growth was performed in the reactor during these tests. Greater details on the experimental investigation are given in reference 5.

The primary purposes of this investigation were to characterize the fluid dynamics of the reactor, and to examine the effects of buoyancy-induced convection. An inlet flow rate of 3 slpm was held constant as the reactor flow was first interrogated at room temperature, then at the typical growth temperature of 700° C. An orthogonal coordinate system was selected to be parallel and perpendicular to the 31 degree inclination of the susceptor face.

The characterization of the reactor flow was determined by measuring the three components of velocity in four planes located parallel to the susceptor face. The results from the plane 6.25 mm above the surface are shown in figures 9 and 10 for the cold and hot flows respectively. Combining measurements obtained along a line displaced 2.5 mm from the centerline of the reactor yields a vertical cross section of the flow. The results are shown in figures 11 and 12 for the cold and hot flows respectively.

Comparison of the results from the two test conditions indicated that the basic reactor design took advantage of significant thermal effects. For CVD applications, the fluid dynamics in the cold flow had several undesirable characteristics. A large scale three-dimensional eddy structure tended to form in the region between the susceptor and the front face of the reactor. The direction of this structure appeared to be controlled by an unstable fluidic attachment of the inlet gas stream to an interior wall of the reactor. The magnitude of the velocity perpendicular to the susceptor surface was found to be low, resulting in poor flow transport toward the surface.

Increasing the temperature of the graphite susceptor to a temperature of 700° C by RF induction changed the flow characteristics considerably. The effects of buoyancy and thermal expansion were found to play a dominant and stabilizing role. The poorly organized flow in the cold reactor was replaced by well directed streamlines with much larger velocity magnitudes. This more organized flow would transport the reactants to the surface more efficiently, resulting in better quality deposition of material.

Global Velocity Measurements of Supersonic Flows

The need for increased aircraft performance and operational efficiency has raised questions about interactions of flow structures with neighboring flows and aircraft structures. Classical methods used in theoretical fluid mechanics and experimental testing relied on closed form solutions validated with sparse probe measurements at various locations within the flow and on the wind tunnel model surface. The advent of computational fluid dynamics (CFD) has increased the understanding of basic fluid mechanics, and has provided insight into complex flows. Unfortunately, standard measurement techniques can not provide the necessary experimental database needed to validate the new codes. The time required to obtain measurements using probes or even fringe-type laser velocimetry raises questions about flow stability and the validity of using point measurements to describe a complete

flow field. This problem becomes worse when considering supersonic flows where wind tunnel run times are typically short.

Recent advances in laser velocimetry, notably particle image velocimetry (PIV)^{9, 10} and Doppler global velocimetry (DGV),^{11, 12} have provided new measurement tools that can provide velocity measurements with spatial coverages and resolutions that rival grid structures in CFD. These devices also have the capability to obtain these measurements in a very short period of time, with sufficient measurement accuracy to provide the necessary experimental database for CFD validation.

The PIV was used at Langley to measure the flow about an oblique shock generated by a 14.5-degree wedge inclined to -15 degrees at Mach 6.13. This test demonstrated the capability of PIV to measure supersonic flows with nominally 1.0 micron Al_2O_3 particles with measurement accuracies rivaling fringe-type laser velocimetry. A photograph of the double exposed particles is shown in figure 13 with the results shown in figure 14. Presently PIV has two characteristics which limit its applicability to general purpose fluid diagnostics. The technique is currently limited to 2-component measurements, and has a limited viewing area in order to maintain sufficient resolution to image the small tracer particles.

While DGV does not appear to have the limitations of PIV, it is still in the development stage. As part of the development program to determine its capabilities and limitations, a series of tests were conducted in the NASA Langley Unitary Plan Wind Tunnel. The DGV was a single component system capable of acquiring analog data at video rates and digital data in individual snapshots. The Argon ion laser output was approximately 1.0 W of single frequency laser power at 514.5 nm. The laser light sheet was obtained using a high-frequency galvanometer system operating at 130 Hz to paint the light sheet on the desired measurement plane. A photograph of the light sheet illuminating water vapor condensation in the tunnel at Mach 2.8 is shown in figure 15. For the first phase of the investigation, the laser light sheet was aligned along the tunnel centerline, inclined by approximately 30 degrees to allow transmission through the side window of the test section. The receiver was placed directly opposite, on the other side of the tunnel to obtain a measure of the vertical velocity component.

The test program began by measuring the vertical component of velocity in the empty tunnel, figures 16 and 17. This data represents an average of 10 frames of video data or approximately 0.33 seconds of acquisition. The sharp decrease in velocity shown in the figures was from the contribution of free stream ($V \sin \alpha$) to the measurements as the laser

beam swept upstream/downstream. If the free stream flow was assumed to be parallel to the tunnel centerline, its contribution to the velocity measurements could be calculated. The corrected data are shown in figures 18 and 19. The remaining velocity distribution indicates a flow structure was present within the test section. This supposition was reinforced by the corresponding measurement standard deviation normalized by free stream shown in figure 20.

In the manner of other laser velocimetry techniques, DGV measures the velocity of tracer particles. The inability of these particles to faithfully follow the gas flow becomes a direct source of measurement error. The simplest method to determine the magnitude of this error in a supersonic flow, was to measure the response of the particles to the sudden velocity change as they pass through an oblique shock. A flat plate was placed in the test section and inclined -15 degrees, and the tunnel run at Mach 2.5. Again, ten frames of data were averaged and the results shown in figure 21. The contribution of free stream to the measurement of the vertical velocity was not removed, so the velocity banding seen in figure 16 was present. The measurement of the velocity profile across the oblique shock is shown in figure 22. The figure also shows the modulation transfer function (MTF) of the CCD video camera. This function is a measure of the spatial response of a CCD to a step change in light intensity, and represents the maximum change in velocity measurable by the DGV. The theoretical velocity profiles, after convolution with the MTF, for 0.5- and 1.0-micron particles are shown in figure 22 for comparison.

The flat plate was then replaced by a 75-degree delta wing set to 24 degrees angle of attack. The laser light sheet was reconfigured to align it perpendicular to the model surface at the 95-percent chord location, figure 15. A second high-speed galvanometer system was placed on the opposite side of the test section to provide a second laser propagation direction. The two light sheets were aligned to the same measurement plane. The receiver was placed downstream to view the light sheet through the side window, first from near the top of the test section, then, for the next tunnel run, lower to align it nearly parallel to the inclined model. During each tunnel run, both galvanometer systems were used to sequentially provide two velocity components. This procedure resulted in the measurement of four separate, but nonorthogonal, velocity components, figures 23 - 26, at a free stream Mach number of 2.8. The optical magnification in the receiver optics restricted the measurement to only the left vortex. The results clearly show the location and internal structure of the vortex, and the shock patterns emanating from it.

Summary

The capability of laser velocimetry to measure extremes in velocity and test conditions has been demonstrated. Fringe-type laser velocimetry was used to measure the intricate Görtler vortices within a laminar boundary layer. It also successfully measured the effects of thermal buoyancy on the flow within a hand-blown fused silica CVD reactor. At the opposite end of the velocity spectrum and measurement requirements, particle image velocimetry provided flow measurements about an oblique shock at Mach 6, and Doppler global velocimetry provided simultaneous measurements of the vortical flow field above a 75-degree delta wing at Mach 2.8. While in some cases, laser velocimetry can be difficult to apply, the present investigations indicate that these efforts can provide insight into complex flows not otherwise obtainable. Also, the advent of global laser velocimetry techniques provides alternatives to the laborious point-measurement approaches for full field investigations.

References

1. Görtler, H.: *Instabilität Laminaren Grenzschichten an Konkaven Wänden Gegenüber Gewissen Dreidimensionalen Störung*. ZAMM Vol. 21., No. 1, 1941, pp. 250-252.
2. Mangalam, S. M.; Dagenhart, J. R.; Hepner, T. E.; and Meyers, J. F.: *The Görtler Instability on an Airfoil*. AIAA 23rd Aerospace Sciences Meeting, paper number AIAA-85-0491, Reno, NV, January 14-17, 1985.
3. Stainback, P. C.; and Owen, F. K.: *Dynamic Flow Quality Measurements in the Langley Low-Turbulence Pressure Tunnel*. AIAA 13th Aerodynamic Testing Conference, paper number AIAA-84-0621, San Diego, CA, March 1984.
4. Meyers, J. F.; and Hepner, T. E.: *Velocity Vector Analysis of a Junction Flow Using a Three-Component Laser Velocimeter*. Proceedings of Second International Symposium on Applications of Laser Anemometry to Fluid Mechanics, paper 3.1, Lisbon, Portugal, July 2-4, 1984.
5. Johnson, E. J.; Hyer, P. V.; Culotta, P. W.; and Clark, I. O.: *Flow Field Velocity Measurements for Nonisothermal Systems*. Proceedings of the SPIE Crystal Growth in Space and Related Optical Diagnostics, Vol. 1557, pp. 168-179, San Diego, CA, July 22-23, 1991.

6. Meyers, J. F.: *Review of Typical Applications - Wind Tunnels*. von Karman Lecture series 1991-08 – Laser Velocimetry, 1991.
7. Talbot, L.; Cheng, R. K.; Schefer, R. W.; and Willis, D. R.: *Thermophoresis of Particles in a Heated Boundary Layer*. J. Fluid Mech. Vol. 101, Part 4, 1980, pp. 737-758.
8. Fotiadis, D. I.; and Jensen, K. F.: *Thermophoresis of Solid Particles in Horizontal Chemical Vapor Deposition Reactors*. J. Crystal Growth, 102, 1990, pp. 743-761.
9. Adrian, R. J.: *Processing Techniques: Image Plane and Fourier Plane*. von Karman Lecture Series 198806, Particle Image Displacement Velocimetry, 1988.
10. Humphreys, W. M.; Bartram, S. M.; and Blackshire, J. L.: *A Survey of Particle Image Velocimetry Applications in Langley Aerospace Facilities*. AIAA 31st Aerospace Sciences Meeting & Exhibit, paper no. AIAA-93-0411, Reno, NV, January 11-14, 1993.
11. Meyers, J. F.; and Komine, H.: *Doppler Global Velocimetry - A New Way to Look at Velocity*. Laser Anemometry: Advances and Applications, 1991, eds. A. Dybbs & B. Ghorashi, ASME
12. Meyers, J. F.; Lee, J. W.; Cavone, K. W.; and Suzuki, K. W.: *Investigation of the Vortical Flow Above an F/A-18 Using Doppler Global Velocimetry*. 5th International Conference on Laser Anemometry - Advances and Applications, Koningshof, Veldhoven, The Netherlands, August 23-27, 1993.
13. Humphreys, W. M., Jr.; Rallo, R. A.; Hunter, W. W., Jr.; Bartram, S. M.; and Blackshire, J. L.: *Application of Particle Image Velocimetry to Mach 6 Flows*. 5th International Conference on Laser Anemometry - Advances and Applications, Koningshof, Veldhoven, The Netherlands, August 23-27, 1993.

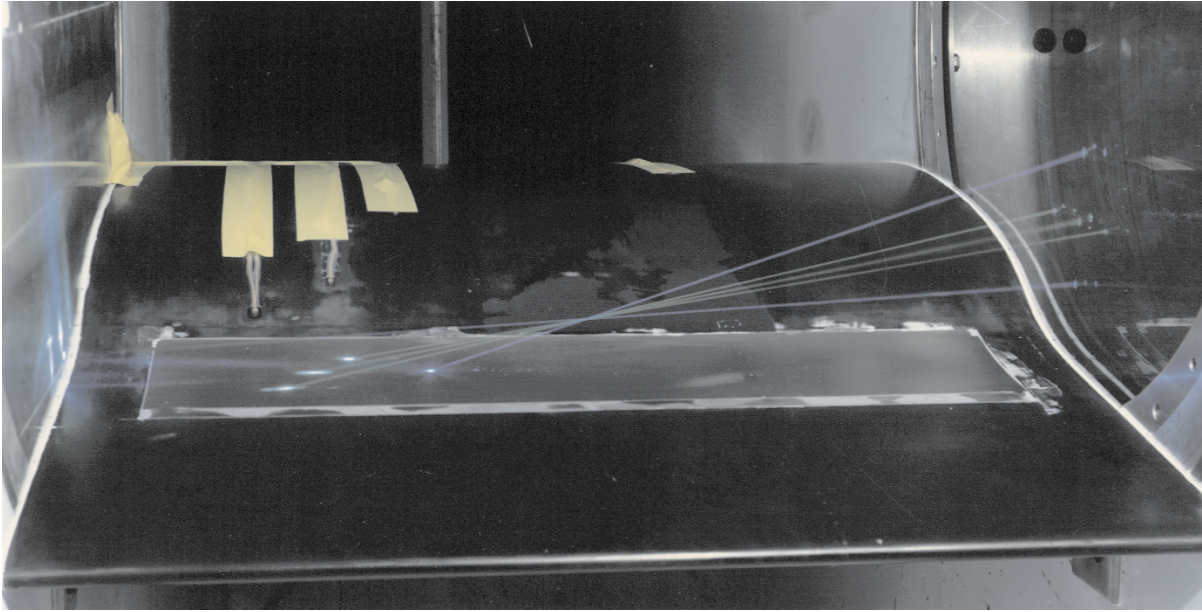


Figure 1.- Görtler model in the Low-Turbulence Pressure Tunnel.

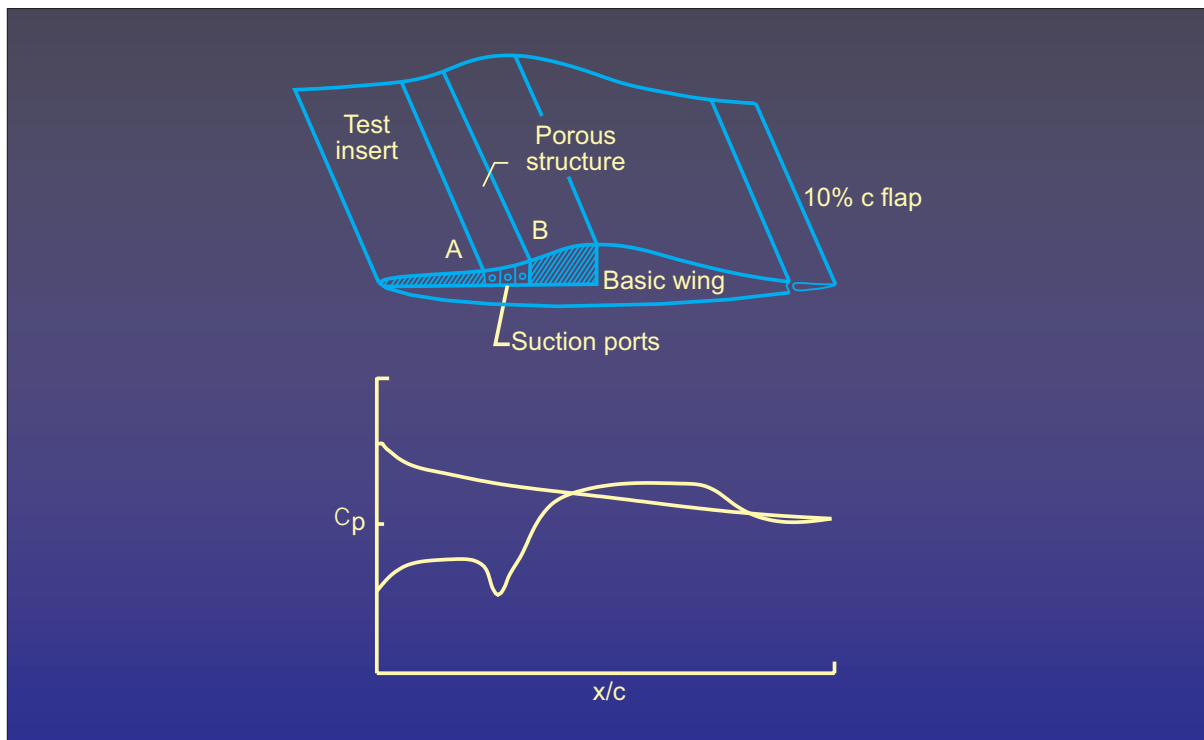


Figure 2.- Model schematic diagram and pressure distribution.

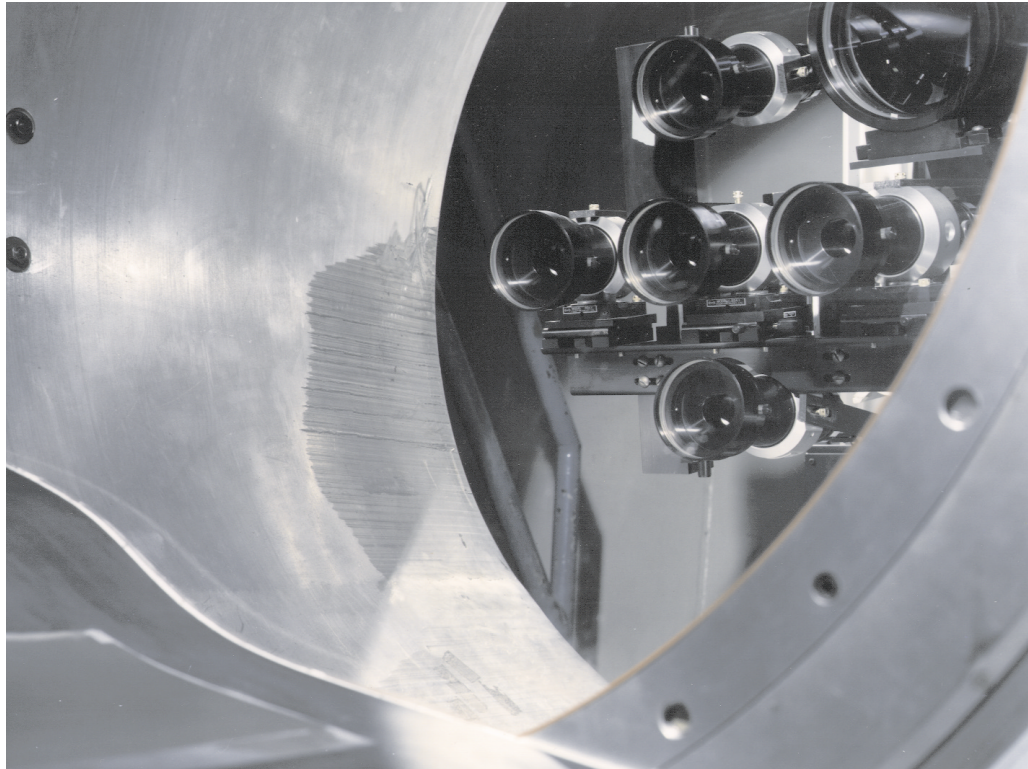


Figure 3.- Laser velocimeter optical system.

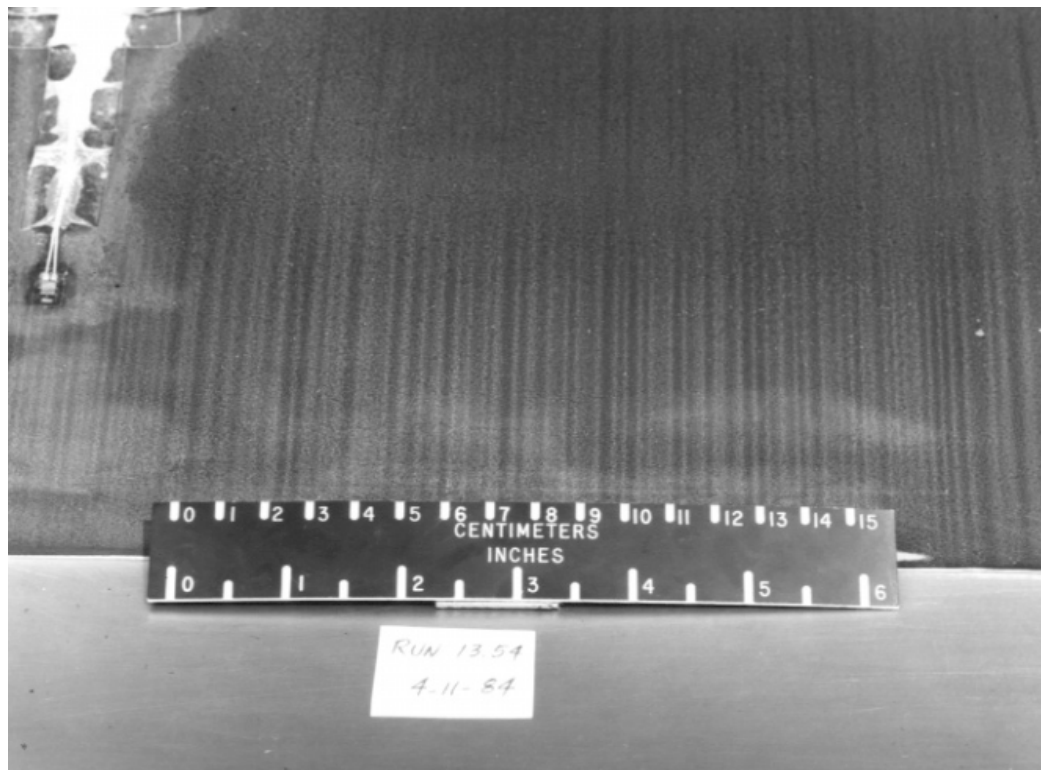


Figure 4.- Flow visualization using sublimating chemicals,
 $M = 0.05$, $R_c = 2.24 \times 10^6$.

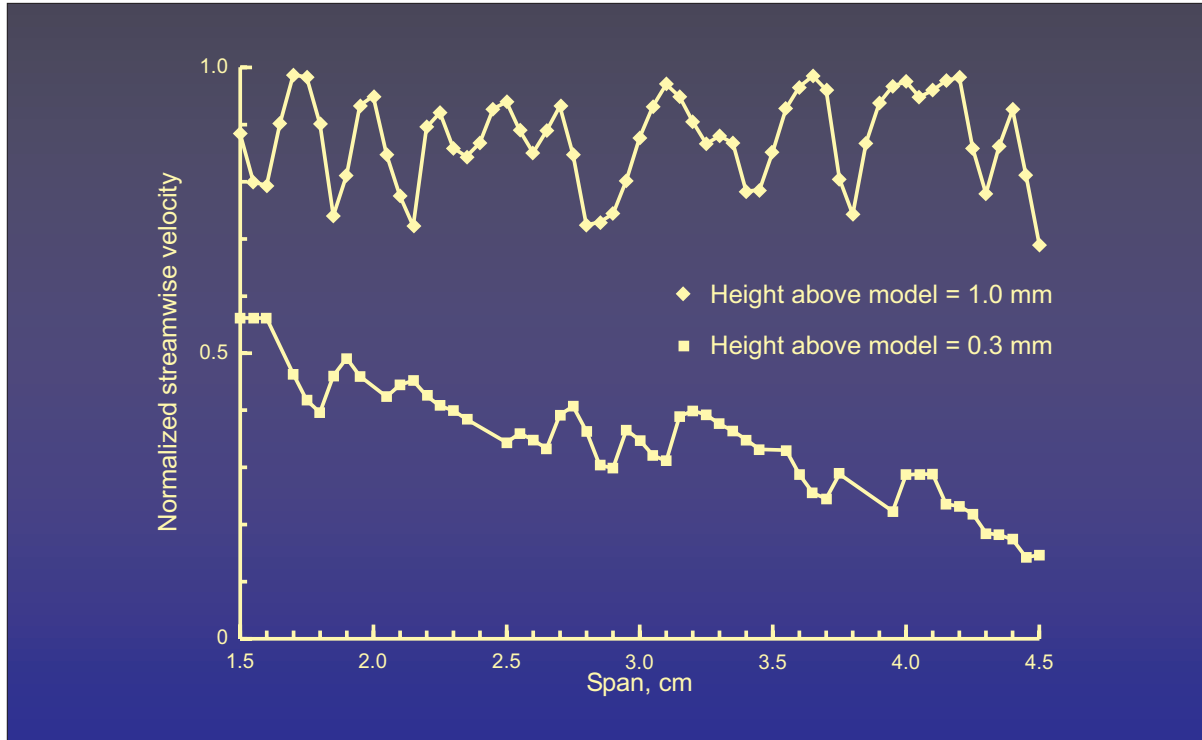


Figure 5.- Spanwise variation of streamwise velocity component,
 $R_c = 2.1 \times 10^6$, $M = 0.05$, $x/c = 0.275$.

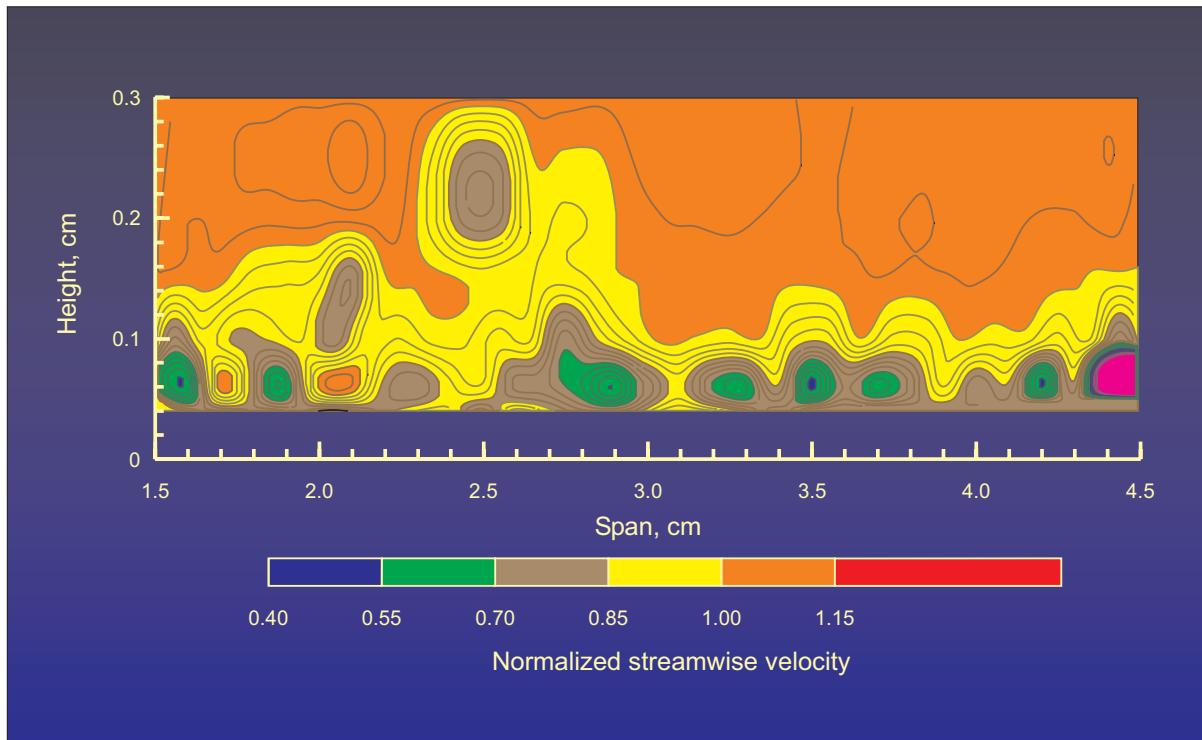


Figure 6.- Flow field map of the Görtler vortices,
 $R_c = 2.1 \times 10^6$, $M = 0.05$, $x/c = 0.275$.



Figure 7.- Chemical Vapor Deposition Facility.

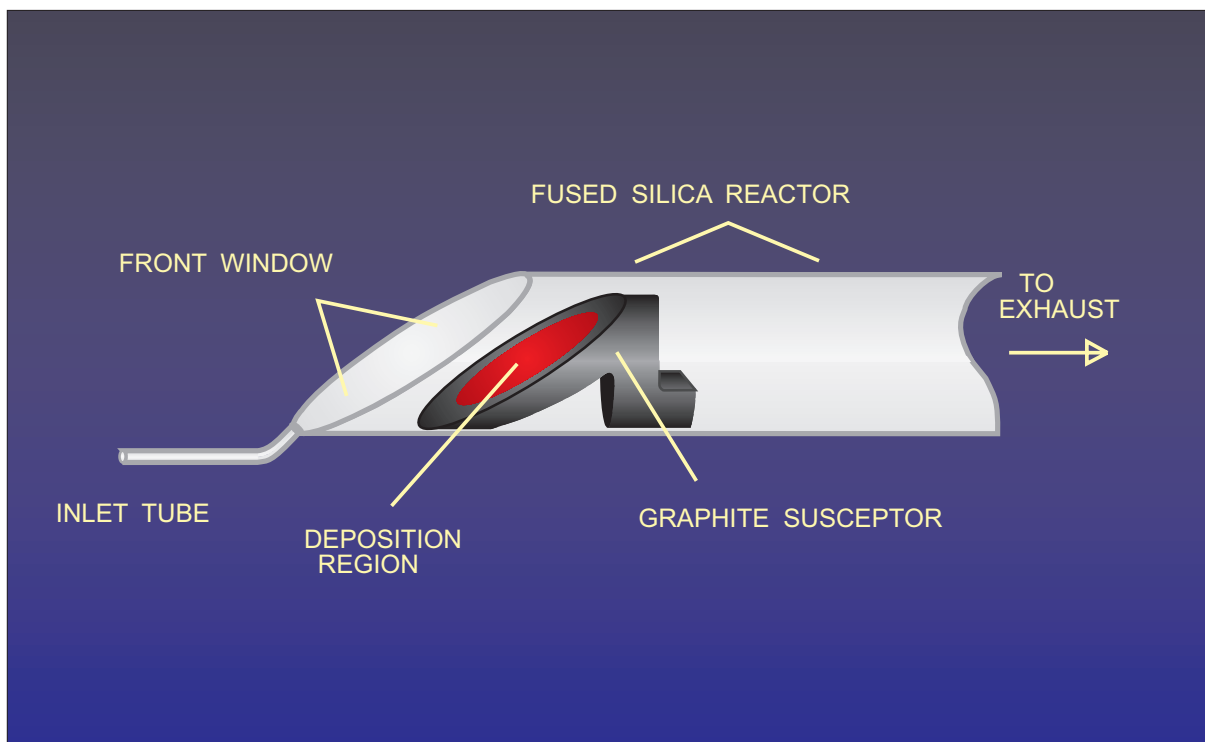


Figure 8.- Reactor configuration showing tilted susceptor and slanted front window.

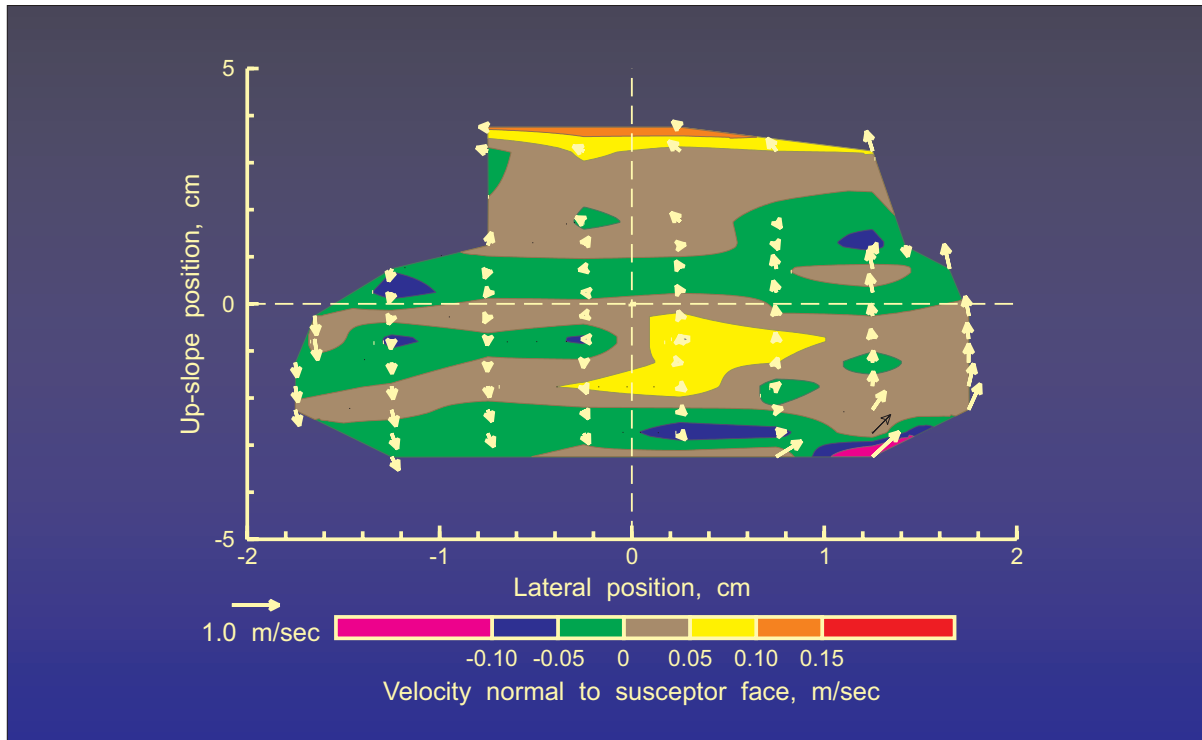


Figure 9.- Cold susceptor: Velocity components measured in a plane parallel to the face of the susceptor at a perpendicular distance of 6.25 mm.

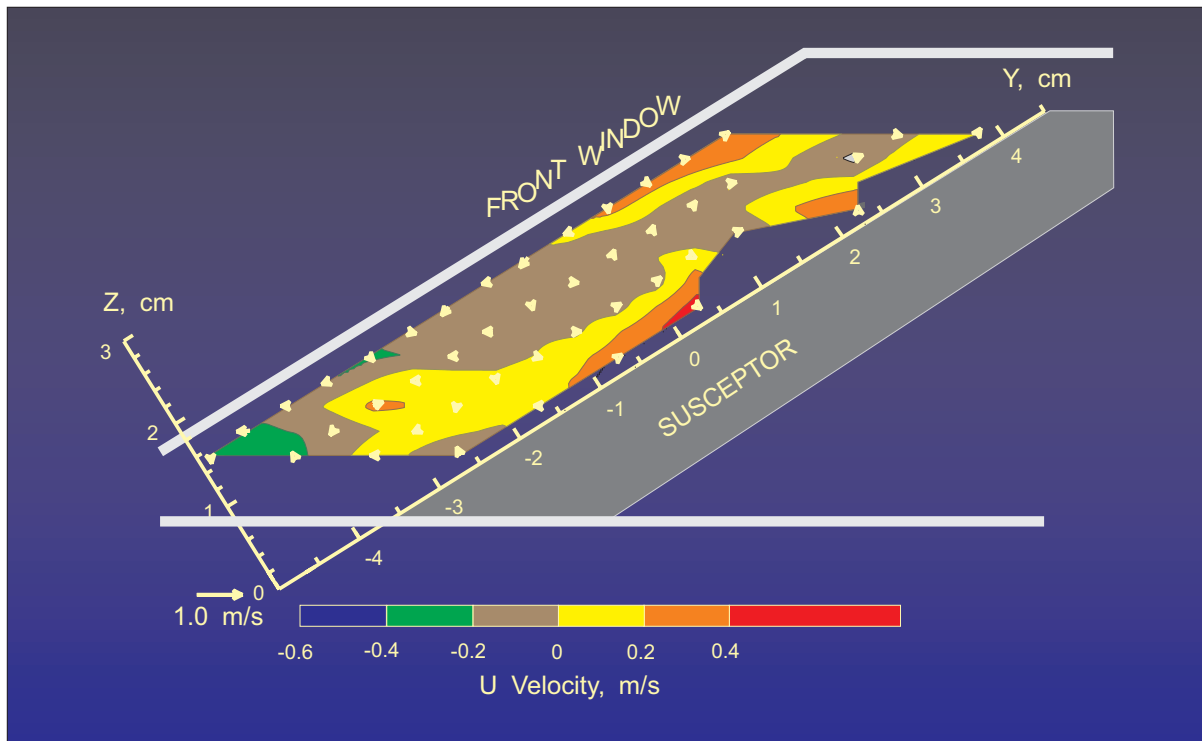


Figure 10.- Cold susceptor: Velocity components measured in a plane normal to the face of the susceptor displaced 2.5 mm from the centerline of the reactor.

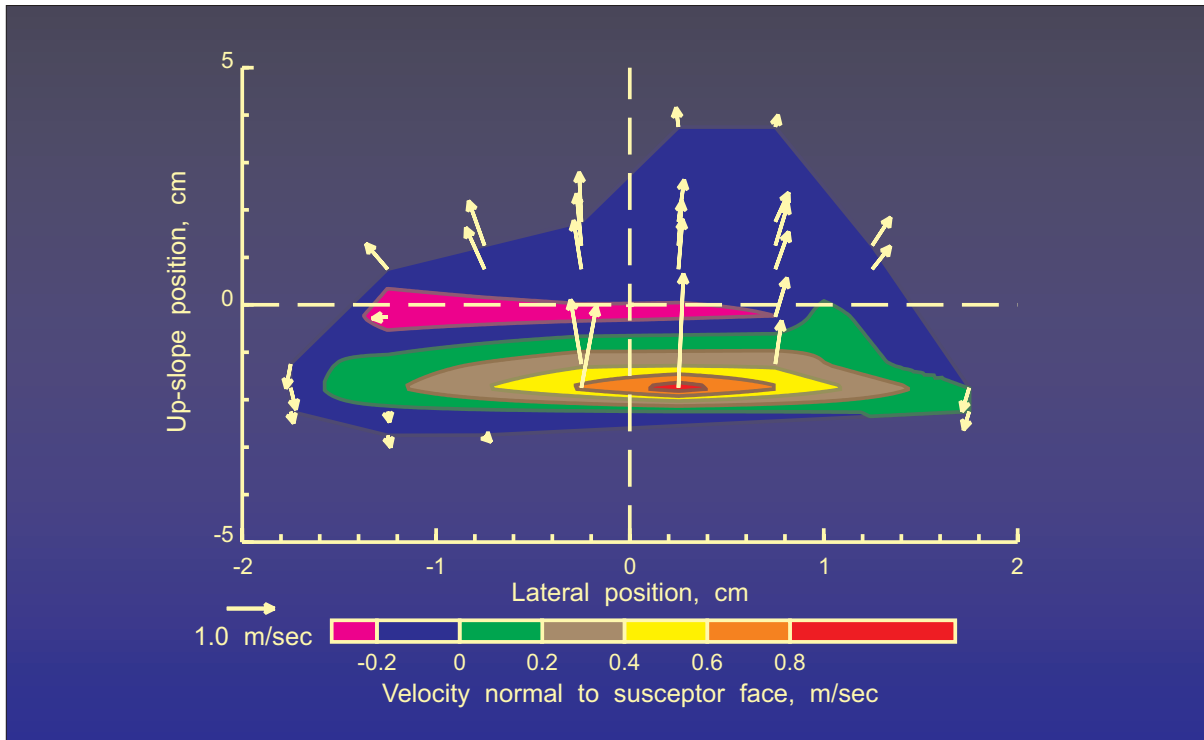


Figure 11.- Hot susceptor: Velocity components measured in a plane parallel to the face of the susceptor at a perpendicular distance of 6.25 mm.

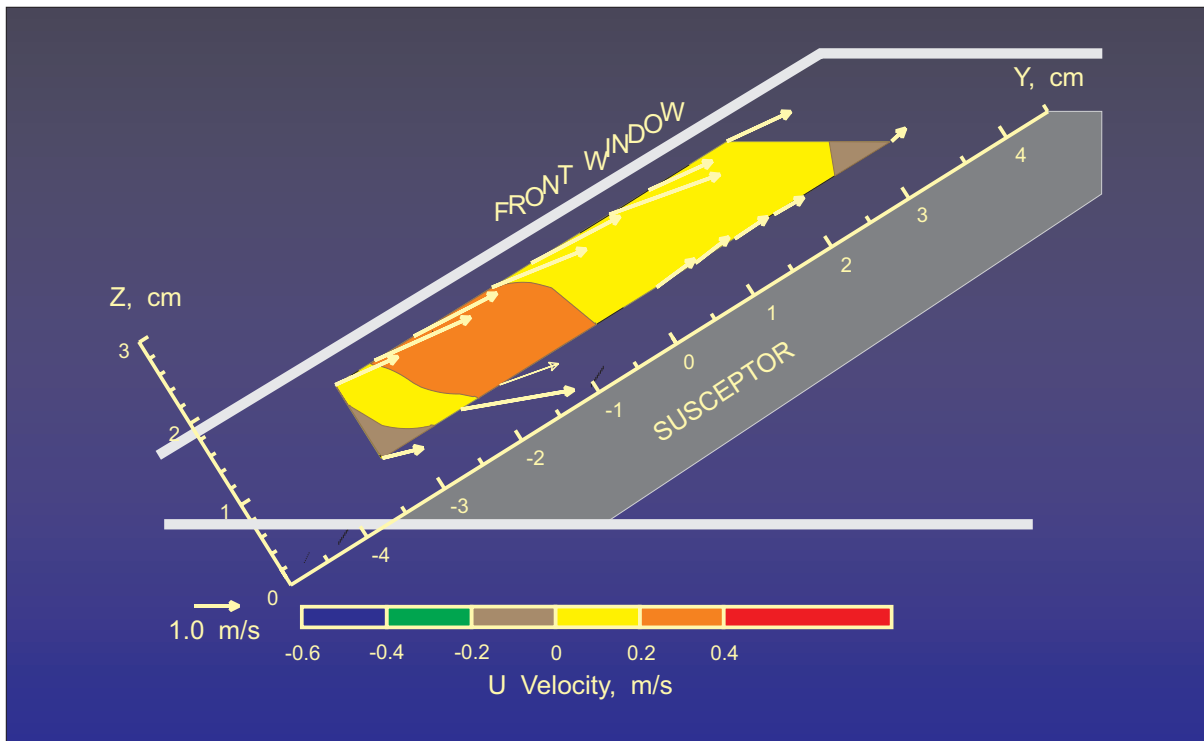


Figure 12.- Hot susceptor: Velocity components measured in a plane normal to the face of the susceptor displaced 2.5 mm from the centerline of the reactor.

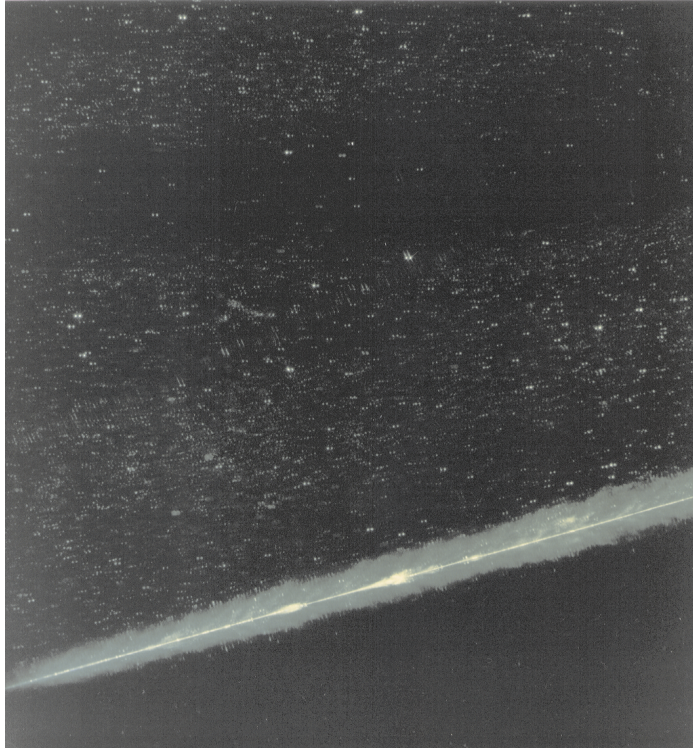


Figure 13.- Double exposed photograph of the particle field above a 14.5-degree wedge at Mach 6.

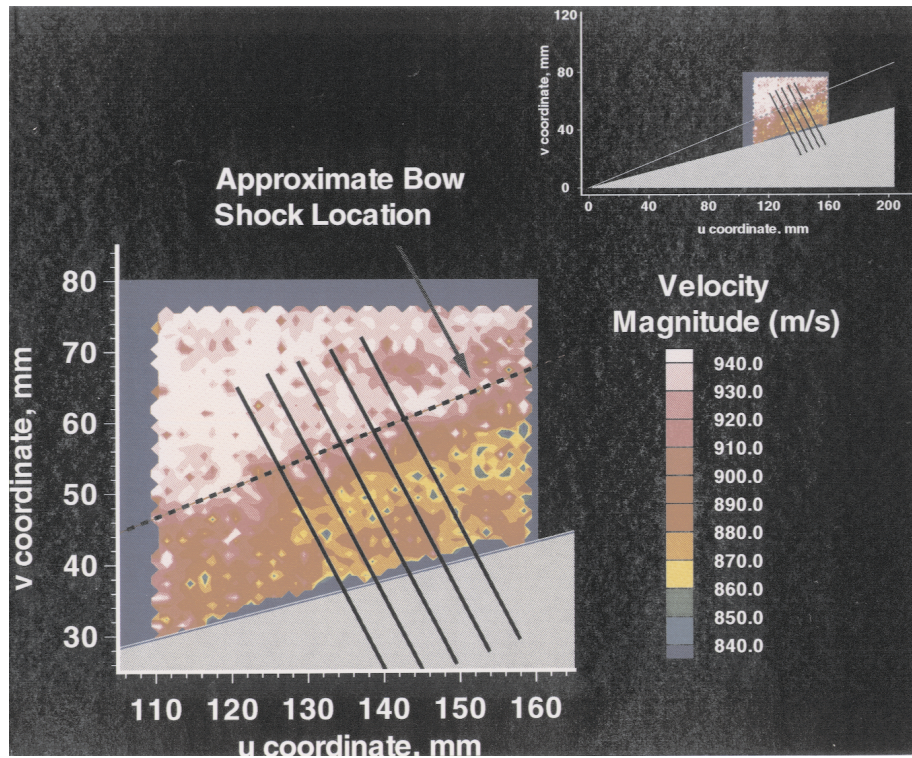


Figure 14.- Map of the velocity magnitude measured by PIV above a 14.5-degree wedge at Mach 6.



Figure 15.- Photograph of the laser light sheet above a 75-degree delta wing at the 95-percent chord location at Mach 2.8.

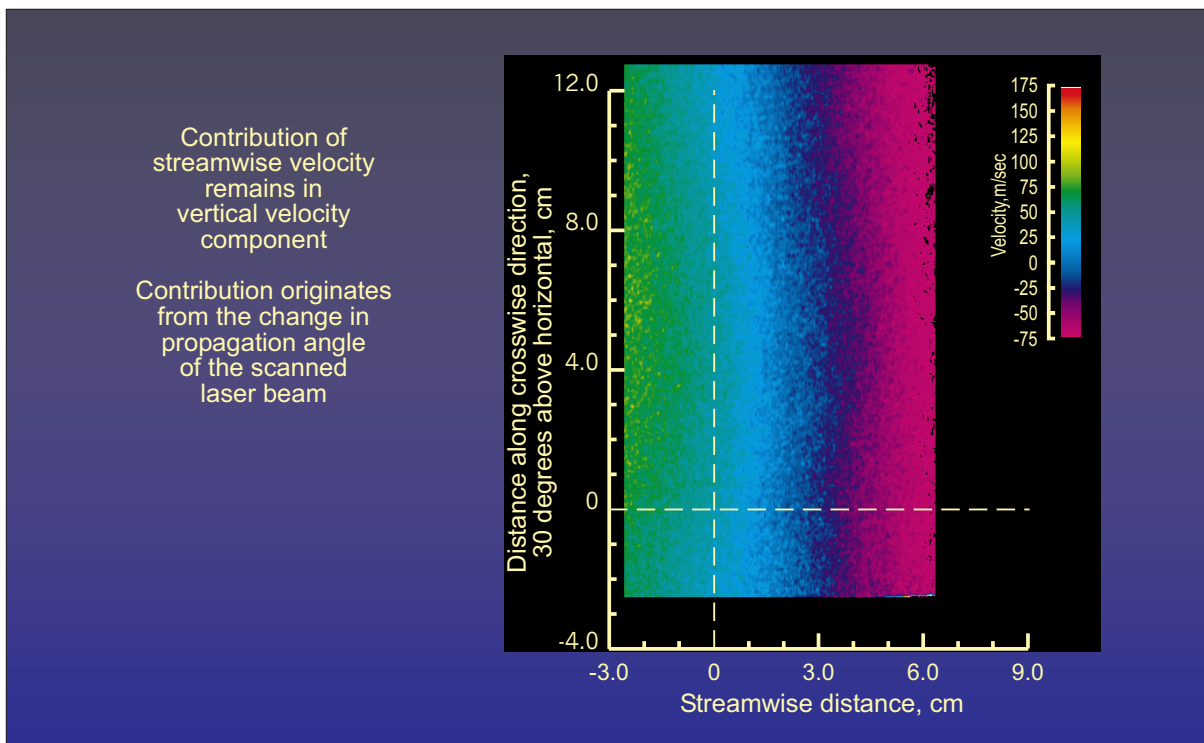


Figure 16.- Map of the vertical velocity component measured by DGV of the empty tunnel flow at Mach 2.5. Streamwise velocity contribution remains in data.

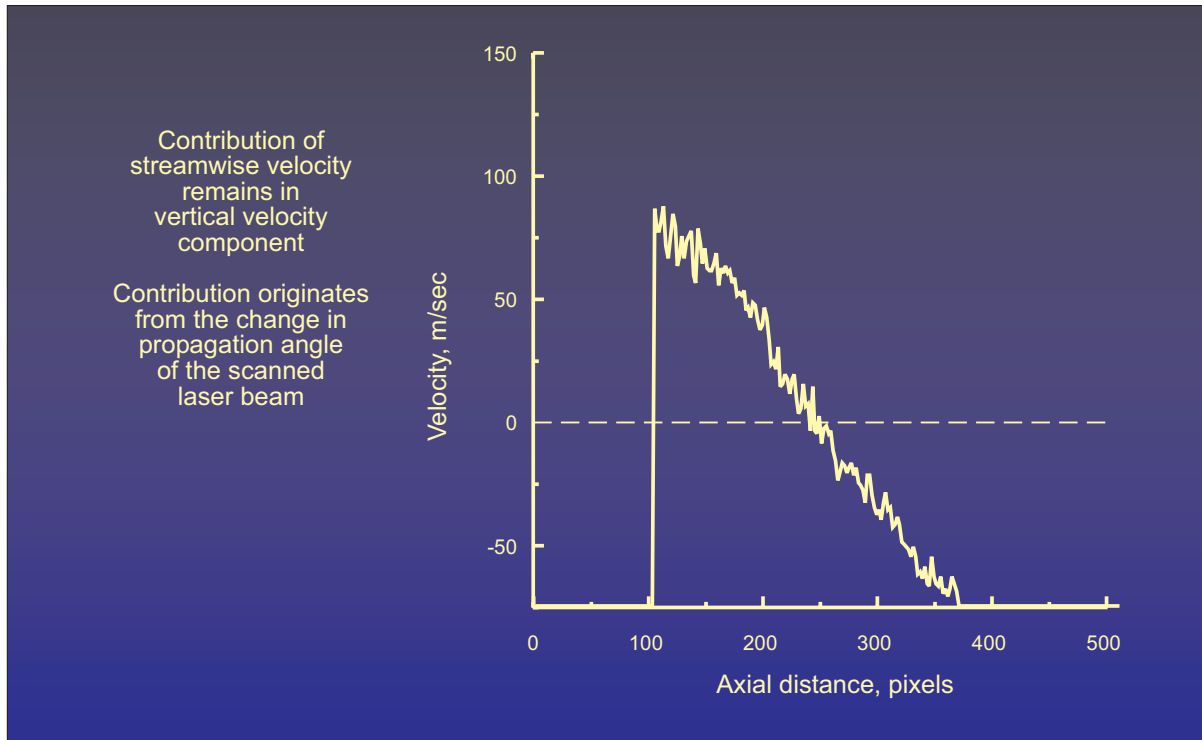


Figure 17.- Streamwise profile of the vertical velocity component measured by DGV of the empty tunnel flow at Mach 2.5. Streamwise velocity contribution remains in data.

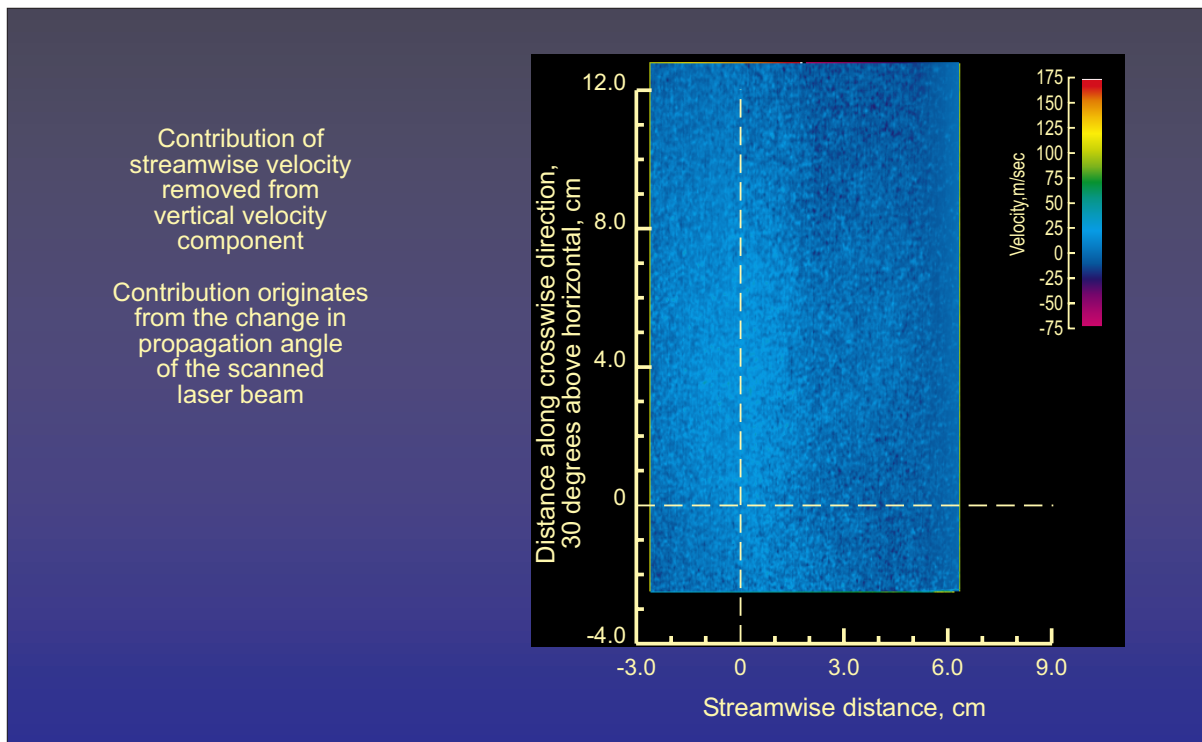


Figure 18.- Map of the vertical velocity component measured by DGV of the empty tunnel flow at Mach 2.5. Streamwise velocity contribution removed.

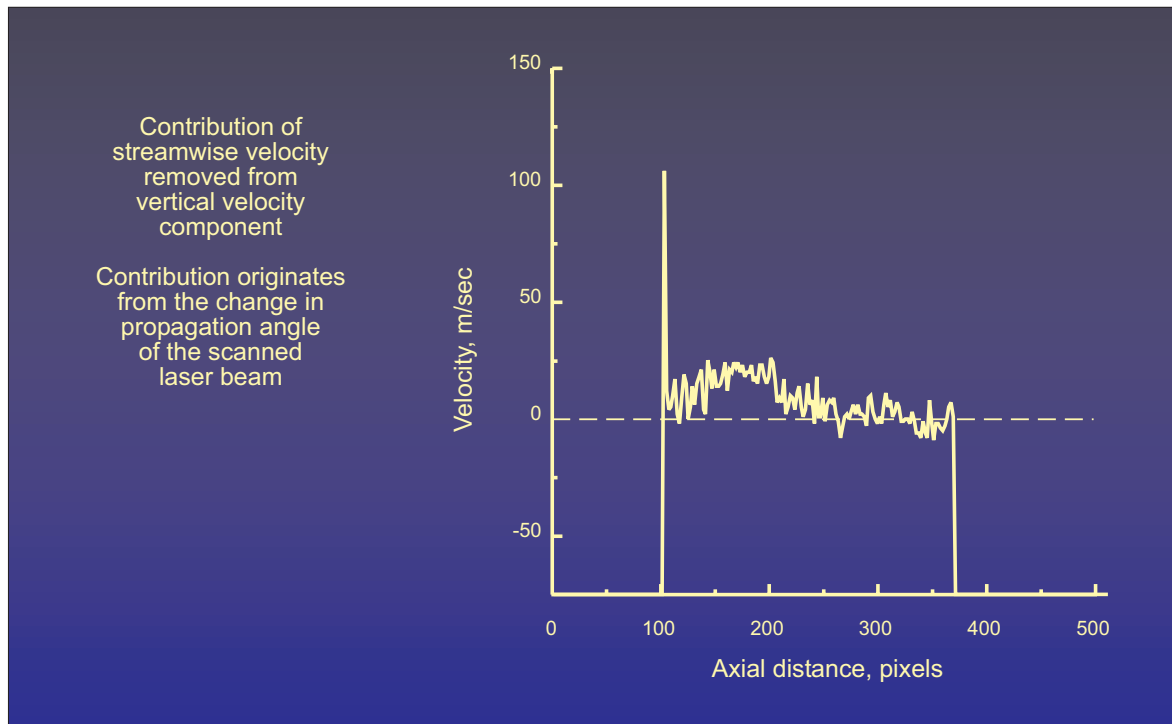


Figure 19.- Streamwise profile of the vertical velocity component measured by DGV of the empty tunnel flow at Mach 2.5. Streamwise velocity contribution removed.

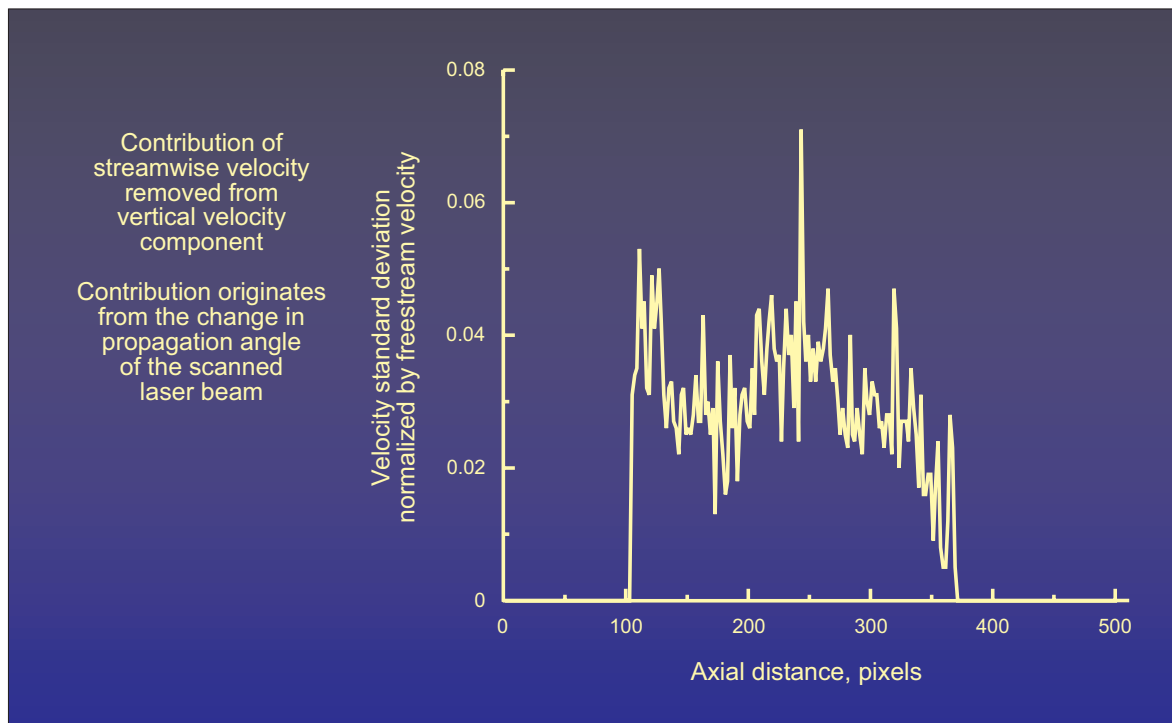


Figure 20.- Streamwise profile of the standard deviation of the DGV measurements of the vertical velocity component normalized by free stream of the empty tunnel flow at Mach 2.5.

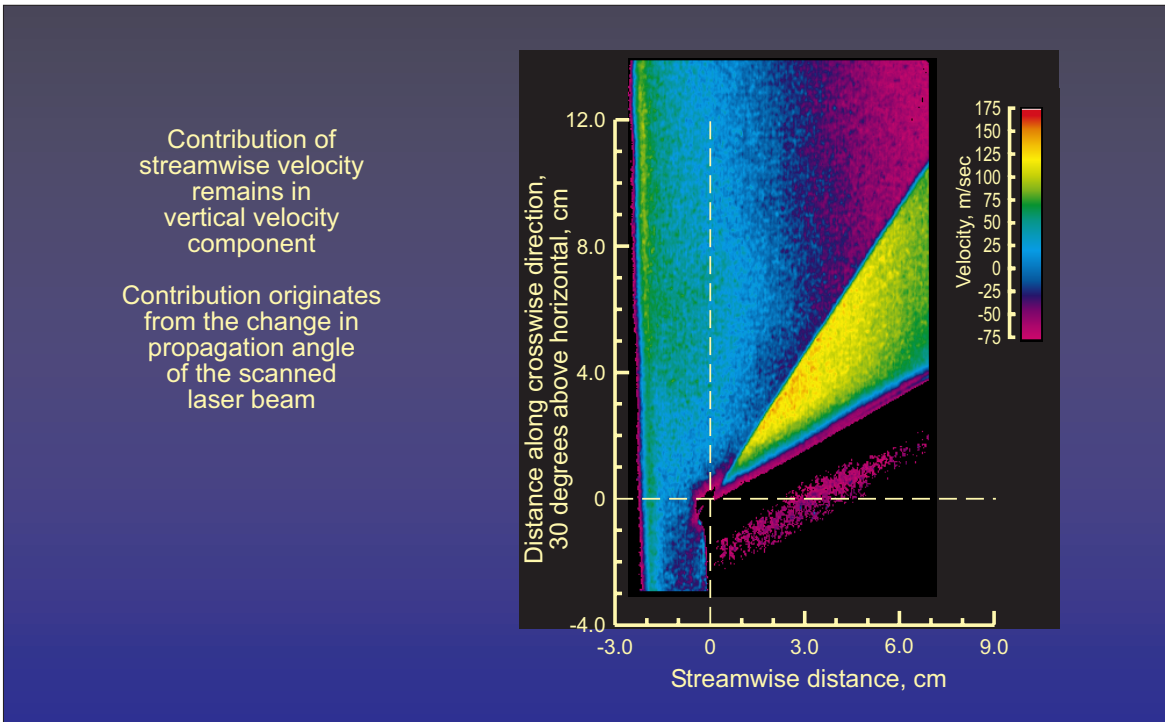


Figure 21.- Map of the vertical velocity component measured by the DGV of the flow above a flat plate inclined to -15 degrees at Mach 2.5. Streamwise velocity contribution remains in data.

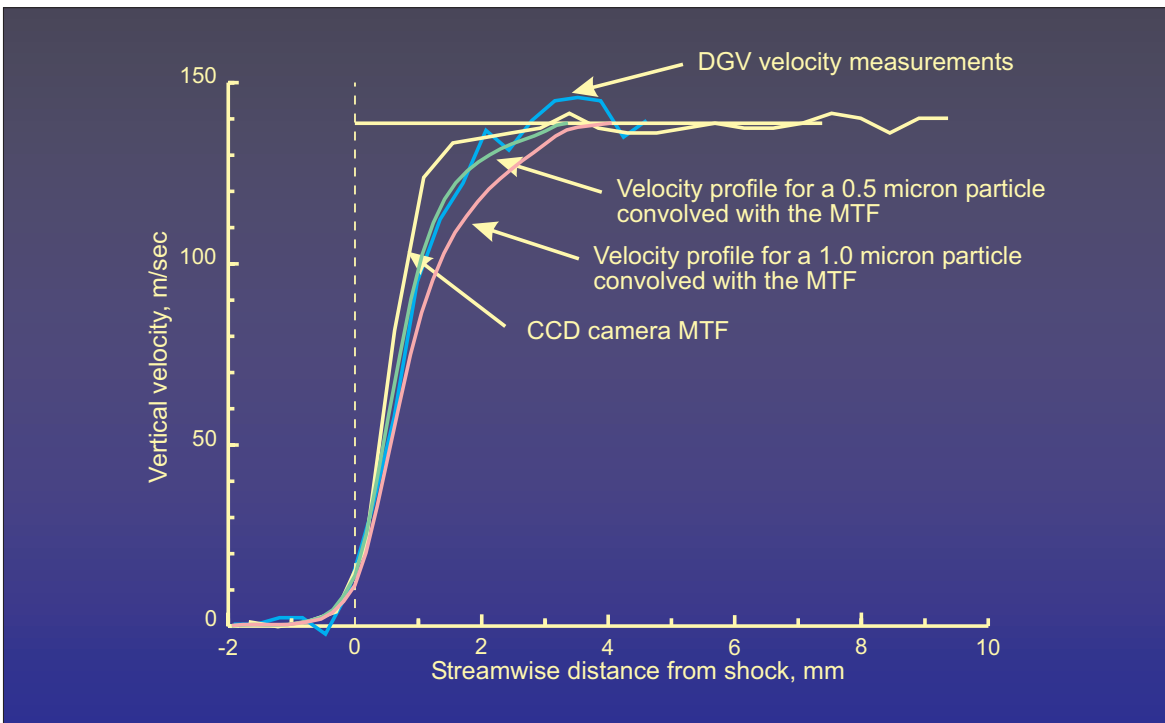


Figure 22.- Comparison of the DGV measurements across the shock with theoretical responses for 0.5 micron and 1.0 micron particles. The CCD camera modulation transfer function indicates the limits of the instrument.

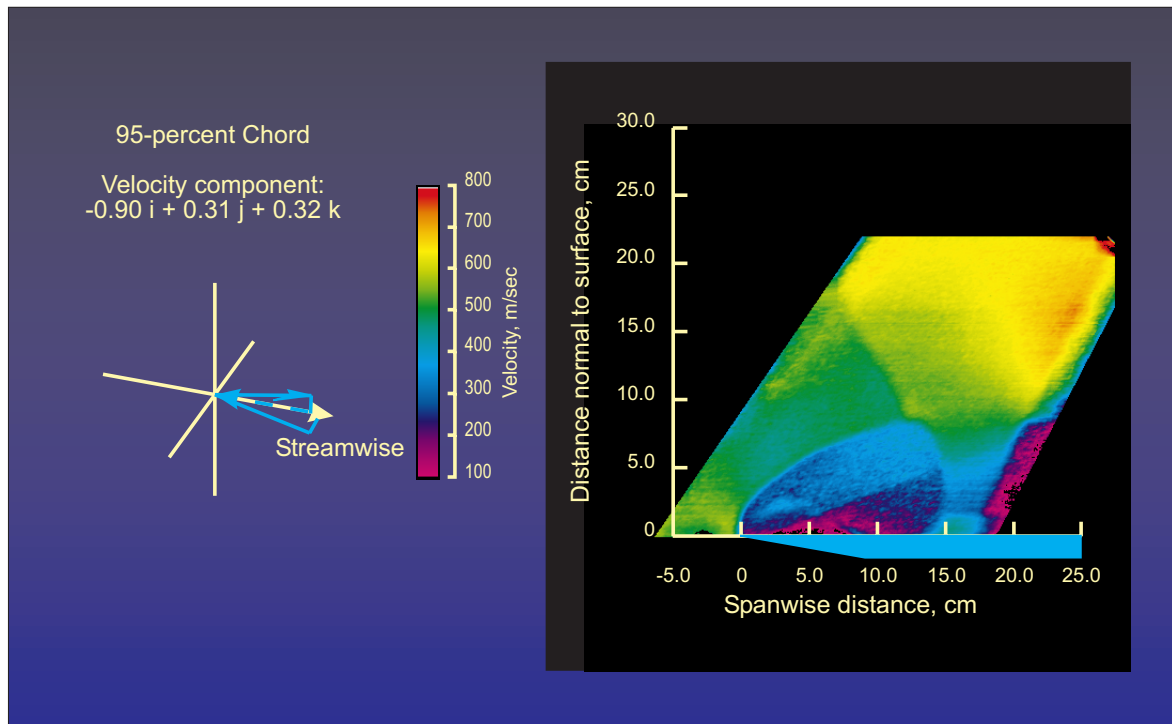


Figure 23.- Map of the velocity component: $-0.90\mathbf{i} + 0.31\mathbf{j} + 0.32\mathbf{k}$ measured by the DGV of the vortical flow above a 75-degree delta wing at the 95-percent chord location at Mach 2.8.

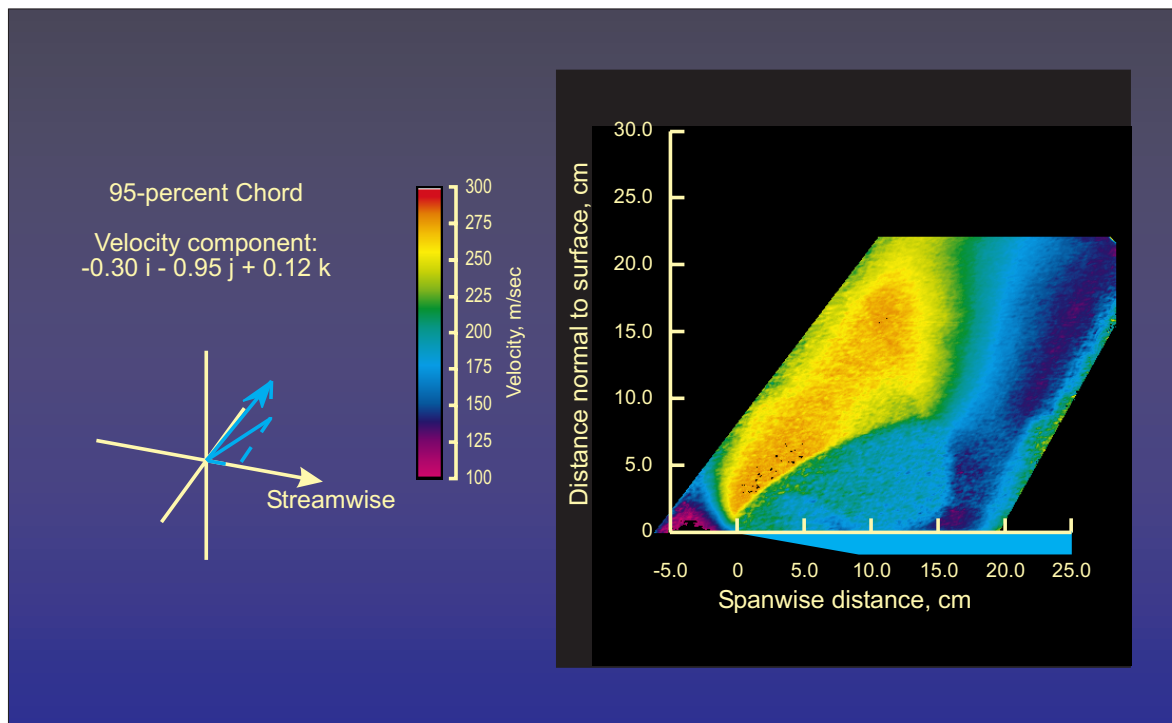


Figure 24.- Map of the velocity component: $-0.30\mathbf{i} - 0.95\mathbf{j} + 0.12\mathbf{k}$ measured by the DGV of the vortical flow above a 75-degree delta wing at the 95-percent chord location at Mach 2.8.

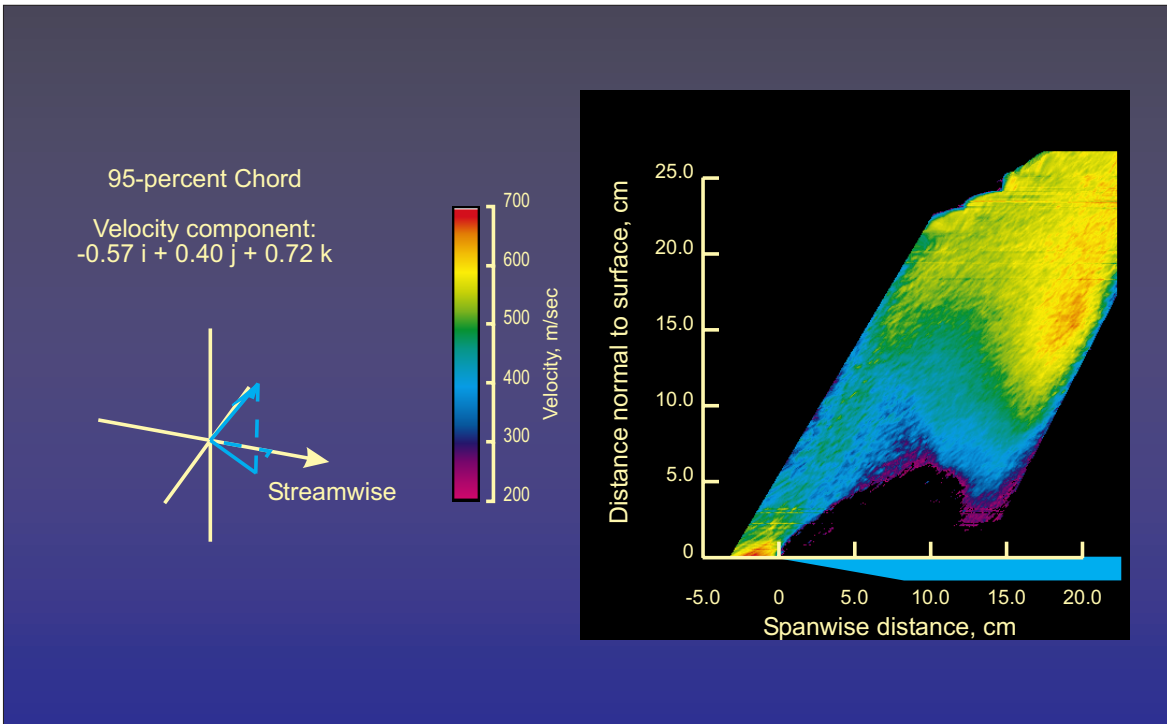


Figure 25.- Map of the velocity component: $-0.57i + 0.40j + 0.72k$ measured by the DGV of the vortical flow above a 75-degree delta wing at the 95-percent chord location at Mach 2.8.

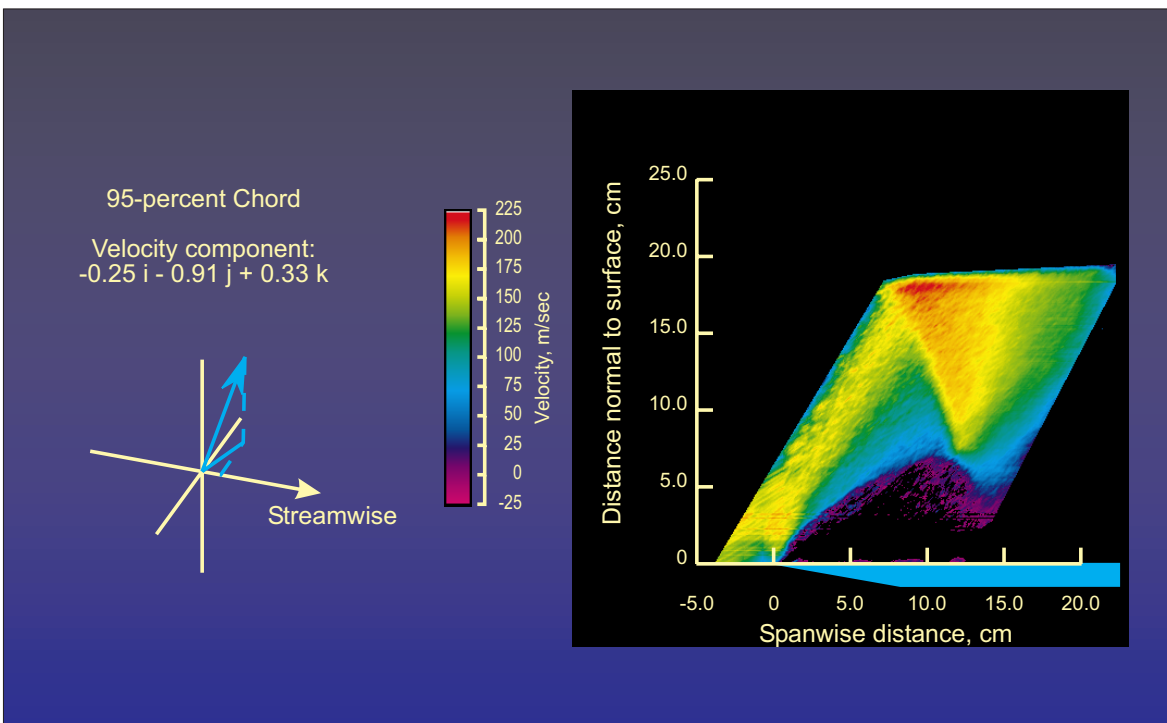


Figure 26.- Map of the velocity component: $-0.25i - 0.91j + 0.33k$ measured by the DGV of the vortical flow above a 75-degree delta wing at the 95-percent chord location at Mach 2.8.